# Coulomb scattering in field and photofield emission

P. J. Donders
*Department of Physics, University of Toronto, Toronto, Canada M5S 1A7*

M. J. G. Lee
*Department of Physics and Scarborough College, University of Toronto, Toronto, Canada M5S 1A7*
(Received 25 September 1986; revised manuscript received 9 March 1987)

An anomalous high-energy tail has been observed in the measured total energy distribution (TED) in photofield emission from tungsten. The strength of this tail is proportional to the product of the photofield emission current and the total emission current. Similar high- and low-energy tails in the TED's in field emission, which have previously been reported by several workers, are also observed. In any given measurement, the fraction of the total photofield-emission current in the anomalous photofield-emission tail is approximately equal to the fraction of the total field-emission current in the anomalous field-emission tail. Measurements of both the absolute strengths and energy dependences of the anomalous tails are reported. The experimental observations are consistent with the predictions of a classical calculation of the energy transfer that results from the Coulomb interaction between electrons in the vacuum near the field emitter. The various internal mechanisms that have previously been invoked to account for the tails in field-emission TED's do not appear to contribute significantly to the anomalous distributions observed in the present work.

## I. INTRODUCTION

According to the established theory of field emission,[1] the total-energy distribution (TED) is expected to decrease exponentially with increasing energy above the Fermi level. However, several investigators[2–7] have observed an anomalous tail in the energy range several eV above the Fermi level, whose strength is proportional to the square of the field-emission current.[2,3] Various mechanisms have been proposed to account for the anomalous tail, including hole-relaxation processes in the bulk,[3] energy broadening due to tunneling lifetimes,[8,9] and energy transfer resulting from Coulomb interactions between the emitted electrons.[10] It has been shown that at high current density the TED of field-emitted electrons is much wider than predicted by the free-electron theory.[10,11] This broadening is due, at least in part, to energy transfer resulting from Coulomb interactions between the emitted electrons.[10,12,13]

In a photofield-emission experiment, a metal surface is illuminated with light having a photon energy smaller than the work function, and a strong static electric field is applied to enable photoexcited electrons to escape either by tunneling through the surface-potential barrier or by passing above it. In the present work it is reported that the TED in photofield emission also has an anomalous high-energy tail which is similar in many respects to the anomalous tail in field emission.

Section II of this paper reports measurements of the anomalous tails in both field and photofield emission. In Sec. III it is shown that the data can be understood in terms of a simple model which takes into account the Coulomb interaction between electrons in the vacuum space close to the tip. The relation of the present observations to previous work in field emission is discussed, and the implications for photofield emission are considered. Finally, in Sec. IV the conclusions of this work are summarized.

## II. EXPERIMENTAL RESULTS

The spectrometer used in the present experiments has been described elsewhere.[14] Electrons emitted from a [110]-oriented tungsten field emitter are accelerated towards a phosphor-coated screen, where they impact to produce a magnified image of the tip. Electrons emitted from a small region of the tip are selected by a probe hole in the screen, decelerated to an average energy of $\sim 1.5$ eV by means of a three-element lens, and then injected into a double-pass 127° cylindrical energy analyzer. The transmitted electrons are detected with a spiraltron electron multiplier. The TED of the emitted electrons can be measured with a resolution of $\sim 60$ meV full width at half maximum.

To generate photoexcited electrons the beam of a krypton-ion laser was focused onto the tip. The photocurrent was maximized by using 351-nm (3.54 eV photon energy) $p$-polarized illumination incident at $\sim 60°$ from the normal of the region of the tip being studied.

Previous work in field emission has shown that the current in the anomalous tail is proportional to the square of the emission-current density.[2] With this in mind, measurements in the present work are from the strongly emitting (310) region of the tip unless otherwise noted.

The TED in field emission predicted by free-electron theory is given by[1]

$$j_f(\varepsilon)=J_f/d\, e^{\varepsilon/d} f(\varepsilon)\ , \tag{1}$$

and the total field-emission-current density is

 

$$J_f = \int_{-\infty}^{\infty} j_f(\varepsilon) d\varepsilon = (4\pi med^2/h^3) e^{-c} , \quad (2)$$

where $\varepsilon$ is the energy relative to the Fermi level, $e$ and $m$ are the electron charge and mass, $h$ is Planck's constant, $1/d = 1.025\Phi^{1/2} t(F,\Phi)/F$ eV$^{-1}$, $f(\varepsilon)$ is the Fermi-Dirac distribution function, $c = 0.68\Phi^{3/2} v(F,\Phi)/F$, $t$ and $v$ are tabulated elliptic functions that account for the image-potential rounding of the surface barrier,[15] $\Phi$ is the work function in eV, and $F$ is the applied electric field in V Å$^{-1}$.

With $p$-polarized illumination the predominant mechanism of photoexcitation is the surface photoeffect,[16] and the free-electron theory[17,18] predicts that the TED in photofield emission, $j_p(\varepsilon)$, has a high-energy tail with energy dependence $e^{\varepsilon(1/d_{\text{eff}} - 1/k_B T)}$, where $k_B$ is Boltzmann's constant and $T$ is the absolute temperature. In the present experiments, $1/d_{\text{eff}} \ll 1/k_B T$ because the final-state energies are close to the peak of the surface-potential barrier.

To test these predictions, a pair of TED's was recorded, one with the tip illuminated and the other with the laser beam blocked. Acquisition of the two TED's was interleaved in time in order to reduce the effects of drift and gradual surface contamination. The measured TED's were severely distorted in the vicinity of the field-emission peak, because the current at the electron multiplier was large enough to cause saturation. To measure the TED's in this energy range, the decelerating lens was defocused so as to reduce the current at the multiplier, and a further pair of TED's was recorded. The two pairs of TED's were normalized with respect to each other using measurements of the TED near $\varepsilon = \hbar\omega$ during illumination before and after defocusing. Separate tests have shown that defocusing the decelerating lens does not significantly alter the measured shape of a TED. Presented in Fig. 1 are the resulting TED's. The photofield-emission TED, which is the difference between the two measured TED's, is also included in the figure.

Both the field-emission and photofield-emission TED's exhibit exponential energy dependences in the energy range immediately above their peaks, as predicted by free-electron theory. From the change in slope of the high-energy tail of the field-emission TED upon laser illumination, it was estimated that the laser-induced tip-temperature rise was 14±3 K at an ambient temperature of ~300 K. Thus laser heating does not significantly populate states more than 0.6 eV (≃20 kT) above the Fermi energy.

The data plotted in Fig. 1 show that both the field-emission and photofield-emission TED's exhibit high-energy tails that extend to energies where free-electron theory predicts negligible emission. It is useful to define $j_f'(\varepsilon)$ to be the TED of the anomalous field emission, and $j_p'(\varepsilon)$ to be the TED of the anomalous photofield emission.

Experiments were performed to determine the dependence of the strength of the anomalous field-emission tail upon the total field-emission-current density, $J_f$. The static electric field dependences of $j_f'(1.08$ eV) and $j_f'(4.62$ eV) were measured over the range 0.30–0.36 V Å$^{-1}$. As a direct measurement of the field dependence of $J_f$ in this field range was impossible due to multiplier saturation, measurements were made of the field dependence of $J_f$ at lower fields, and Eq. (2) was used to extrapolate to the range of interest. The results, which are plotted in Fig. 2, demonstrate that $j_f'$ is proportional to $J_f^2$, in agreement with previous investigations.[2,3] Thus the TED of the anomalous field emission can be can be expressed in the form

$$j_f'(\varepsilon) = \kappa(\varepsilon) J_f^2 . \quad (3)$$

Determining $\kappa(\varepsilon)$ involves estimating the absolute value of $J_f$, in the region of the field emitter that is imaged onto the probe hole. A Fowler-Nordheim analysis of measurements of $J_f$ as a function of the screen potential gave $\beta = 1.02\times10^{-4}$ Å$^{-1}$ ($\beta$ is the ratio of the static electric field at the emitting surface to the screen potential). From this the tip radius is estimated to be[19] $r_{\text{tip}} \simeq (5\beta)^{-1} = 2000$ Å. At a field of 0.32 V Å$^{-1}$ the whole tip field-emission current was $9.0\times10^{-8}$ A. An examination of the field-emission pattern showed that approximately 90% of the whole tip field-emission current comes from the neighborhood of the two (310) regions, and that these regions have a combined area of $6\times10^5$ Å$^2$. Hence $J_f \simeq 1.5\times10^{-13}$ A Å$^{-2}$. Moreover, analysis of the TED measured in a field of 0.32 V Å$^{-1}$ gave $j_f'(1.08$ eV$)/J_f = 5.6\times10^{-5}$ eV$^{-1}$. Using Eq. (3) to combine these results, it follows that $\kappa(1.08$ eV$) \simeq 4\times10^8$ Å$^2$ A$^{-1}$ eV$^{-1}$.

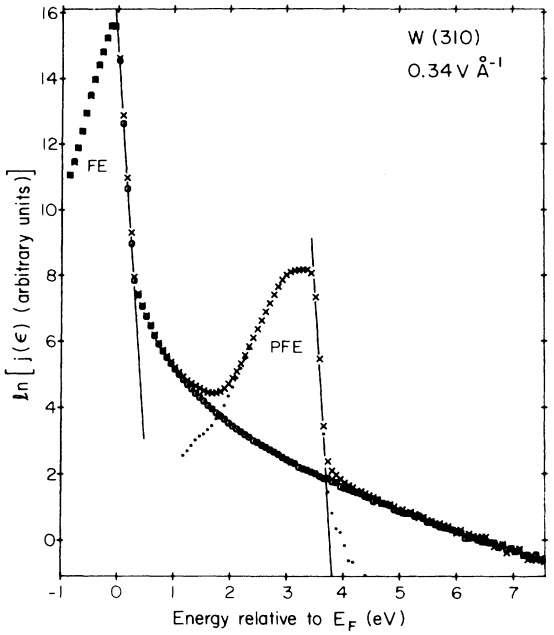


FIG. 1. Plot of the total-energy distribution, $j(\varepsilon)$ of electrons emitted from the (310) region of a tungsten tip at a field of 0.34 V Å$^{-1}$. The crosses are data taken from an illuminated field emitter, the open circles are data taken in the absence of laser illumination, and the solid dots are the difference between these two sets of data, $j_p(\varepsilon)$. The solid lines fitted in the region of the emission peaks are the predictions of the free-electron theory of electron emission.

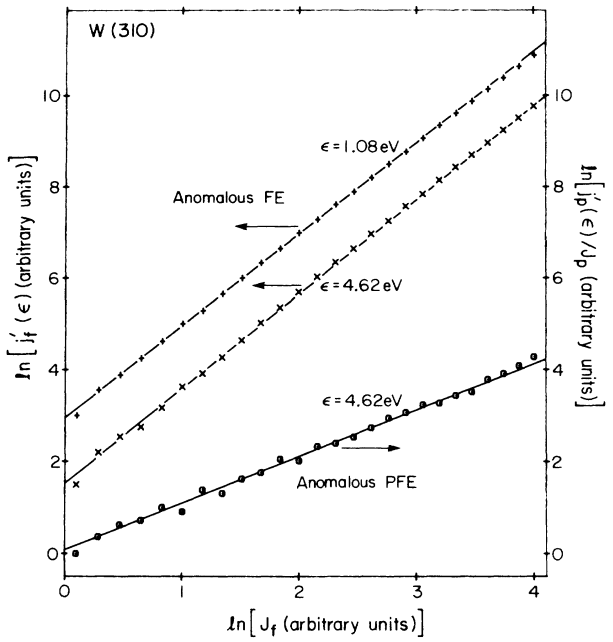


FIG. 2. Log-log plot of the dependence of the anomalous current on the total emission current. The measured values of $j_f'(1.08\ \text{eV})$ are indicated by pluses and those of $j_p'(4.62\ \text{eV})$ are indicated by crosses. The open circles are the measured values of $j_p'(4.62\ \text{eV})/J_p$. For the purpose of comparison, lines of slope 2 are drawn through the field-emission data, and a line of slope 1 is drawn through the photofield-emission data.

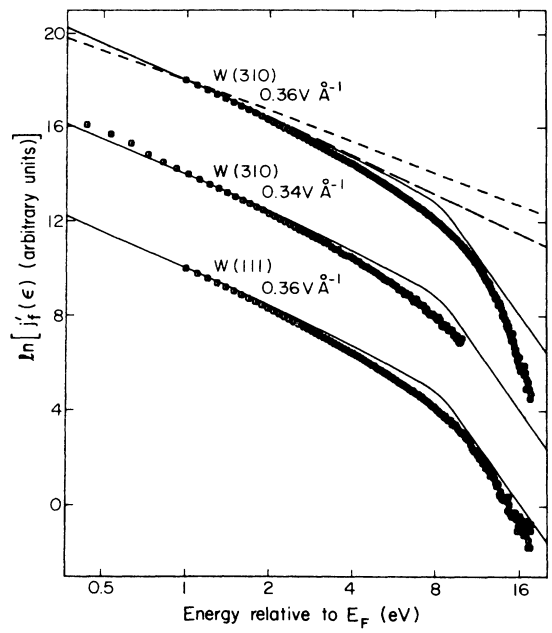


FIG. 3. Log-log plot of the high-energy tails in field emission. Upper curve, (310) region at 0.36 V Å$^{-1}$; middle curve, (310) region at 0.34 V Å$^{-1}$; lower curve, (111) region at 0.36 V Å$^{-1}$. The short-dashed curve is the prediction of the tunneling-lifetime model (Ref. 8). The long-dashed curve is the prediction of the Coulomb-interaction model when no account is taken of the perturbation of the electron trajectories, and the solid curves are the predictions of the Coulomb-interaction model including the perturbation of electron trajectories. For convenience of presentation, all curves have been shifted vertically by arbitrary amounts.

Additional experiments were performed to measure $j_f'(\varepsilon)$ in the range $\varepsilon \geq 5.0$ eV. Experimental results from the (310) and (111) regions of the tip are plotted in Fig. 3. It is seen that for $0.4 < \varepsilon < 4.0$ eV the data exhibit $\sim \varepsilon^{-2.6}$ energy dependence, and that for $\varepsilon > 4.0$ eV the data deviate progressively from this power-law dependence. It is remarkable that even 16 eV above the Fermi level there is a detectable current in the anomalous field-emission tail.

An experiment was performed to look for a possible low-energy tail in field emission whose strength varies as $J_f^2$. Measurements were confined to the region $\varepsilon < -2.5$ eV where, over the field range investigated, the free-electron theory predicts negligible emission. The dependences on static fields of $j_f(-5.20\ \text{eV})$ and $j_f(4.80\ \text{eV})$ were measured in the range 0.32–0.38 V Å$^{-1}$. Once again, $J_f$ was deduced by extrapolation of measurements at low field. If it is assumed that $j_f(\varepsilon) = \alpha J_f + \eta J_f^2$, then a plot of $j_f(\varepsilon)/J_f$ against $J_f$ will yield a straight line of slope $\eta$. Figure 4 shows that the data exhibit precisely this behavior. The low-energy tail has a significant component that is linear in $J_f$, which is probably due to electron scattering at the walls of the analyzer. Supporting this interpretation is the observation that the strength of the linear component relative to the emission current at the peak of the field-emission TED depends on how the analyzer is aligned. There is no significant component of the high-energy tail that is linear in $J_f$, whereas both the high- and low-energy tails of the TED have an anomalous component whose strength is quadratic in $J_f$. Measure-

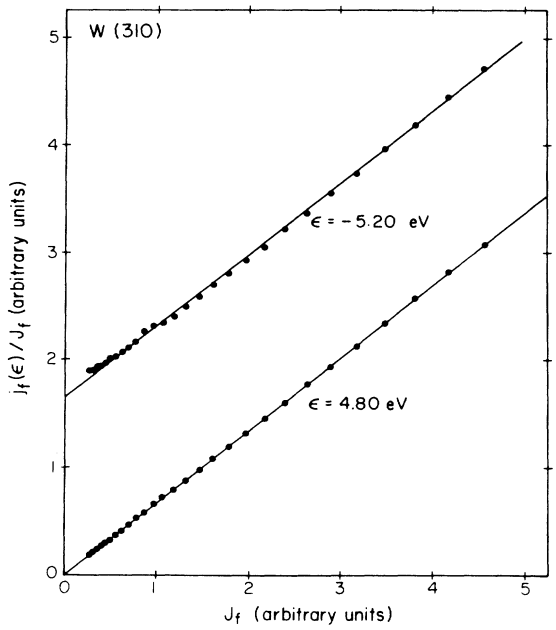


FIG. 4. Plot of $j_f(\varepsilon)/J_f$ as a function of $J_f$. Data are for energies well above (upper curve) and well below (lower curve) the Fermi energy. The slope of these curves is a measure of the anomalous field emission.

ments of the slopes of the two curves in Fig. 4 give $j_f'(-5.20\ \text{eV})/j_f'(4.80\ \text{eV})=0.98\pm0.05$. Since the ratio of the anomalous field-emission current to the background is typically $\sim 10^5$ in the high-energy tail and less than 3 in the low-energy tail, it is possible to study the high-energy tail in much greater detail than the low-energy tail.

An experiment was performed to investigate the influence of tip temperature on the anomalous high-energy tail in field emission. Measurements were performed on the (111) region at a field of 0.33 V Å$^{-1}$. The tip was heated by means of a laser, operating at 647 nm, focused on the shank. Two data sets were acquired, one with the tip illuminated, the other with the laser beam blocked. Raising the tip from 300 to 720 K increased $j_f'(3.18\ \text{eV})$ by $(43\pm4)\%$, and integration of the TED's showed that the square of the field-emission current increased by $(40\pm1)\%$. The consistency between these results suggests that $\kappa(\varepsilon)$ is independent of tip temperature.

The change in the field-emission TED that results from laser-induced heating must be taken into account in determining the TED in photofield emission. In the energy range of the anomalous photofield-emission tail, the only significant field emission is that associated with the anomalous tail. Since $\kappa(\varepsilon)$ is essentially independent of temperature, $j_f'(\varepsilon)$ during laser illumination can be determined from Eq. (3) by combining a measurement of $j_f'(\varepsilon)$ in the absence of illumination with measurements of $J_f$ with and without laser illumination. $j_p'(\varepsilon)$ is the difference between the TED measured during illumination and $j_f'(\varepsilon)$ during illumination. In the majority of experiments reported in the present work, the laser-induced change in $j_f'(\varepsilon)$ is less than 5% of $j_p'(\varepsilon)$.

The relationship between the anomalous photocurrent and the current density in photofield emission, $J_p$, was investigated. During these measurements the laser intensity was set so that the maximum laser-induced tip-temperature rise was $\simeq 15$ K, and the electric field strength was chosen so that at maximum intensity $J_f \sim 60 J_p$. A Pockels cell followed by a linear polarizer was used to control the irradiance at the field emitter. Both $j_p'(4.62\ \text{eV})$ and $j_p(3.44\ \text{eV})$, the latter being proportional to $J_p$, were measured as a function of the potential applied to the Pockels cell. The resulting data, plotted in Fig. 5, demonstrate that $j_p'(\varepsilon)$ is proportional to $J_p$ when $J_f$ is held constant and $J_f \gg J_p$.

The dependence of the anomalous photocurrent upon the total current density in field emission was studied. During these measurements the irradiance was held constant so as to yield a laser-induced tip-temperature rise of $\sim 15$ K, and the electric field strength was varied in a range such that $J_f > 10 J_p$. The static electric field dependences of both $j_p'(4.62\ \text{eV})$ and $j_p(3.44\ \text{eV})$, the latter being proportional to $J_p$, were measured over the range 0.3–0.36 V Å$^{-1}$. Over this range $J_f$ increased by a factor of $\sim 60$ and $J_p$ increased by a factor of $\sim 1.3$. The results, which are plotted in Fig. 2, show that $j_p'/J_p$ is proportional to $J_f$ when $J_f \gg J_p$.

The observations reported above suggest that if $J_p \gg J_f$, then $j_p'$ will be proportional to $J_p^2$. A search for this effect was performed at a field of 0.22 V Å$^{-1}$, and using illumination at close to the maximum available power density ($\sim 1$ GW m$^{-2}$). Under these conditions, $J_p \simeq 40 J_f$. A Pockels cell was used to control the polarization of the laser and, hence, $J_p$.[16] An increase of $J_p^2$ by a factor of $5.1\pm0.1$ was accompanied by an increase in $j_p'(\hbar\omega+2.10\ \text{eV})$ by a factor of $4.9\pm0.3$. The consistency between these results suggests that there is a component of $j_p'$ proportional to $J_p^2$. Combining this conclusion with those of the two preceding paragraphs suggests that the TED of the anomalous photofield emission may be expressed as

$$j_p'(\varepsilon)=\kappa(\varepsilon-\hbar\omega)J_p[\gamma(\varepsilon)J_f+\gamma_{pp}(\varepsilon)J_p]\ . \tag{4}$$

The term involving $\gamma(\varepsilon)$ includes two contributions, one arising from photofield-emitted electrons shifted in energy as a result of scattering by field-emitted electrons, and the other arising from field-emitted electrons shifted in energy as a result of scattering by photofield-emitted electrons. These two contributions cannot be distinguished by experiment.

The ratio $\gamma_{pp}/\gamma$ was determined at a fixed energy. The irradiance at the tip was close to the maximum available, and a Pockels cell was used to control $J_p$. The polarization dependence of $j_p'(4.62\ \text{eV})$ was measured at an applied electric field of $\sim 0.28$ V Å$^{-1}$, as were TED's in the energy range of the peaks. Equation (4) predicts that a plot of $j_p'/(J_p J_f)$ against $J_p/J_f$ will be a straight line, from which $\gamma_{pp}/\gamma$ can be deduced. Representative data plotted in Fig. 6 are consistent with this prediction. The average of several measurements showed that, for emission from the (310) region, $\gamma_{pp}(4.62\ \text{eV})/\gamma(4.62\ \text{eV})=1.50\pm0.08$, while for emission from the (111) region, $\gamma_{pp}(4.62\ \text{eV})/\gamma(4.62\ \text{eV})=0.93\pm0.13$.

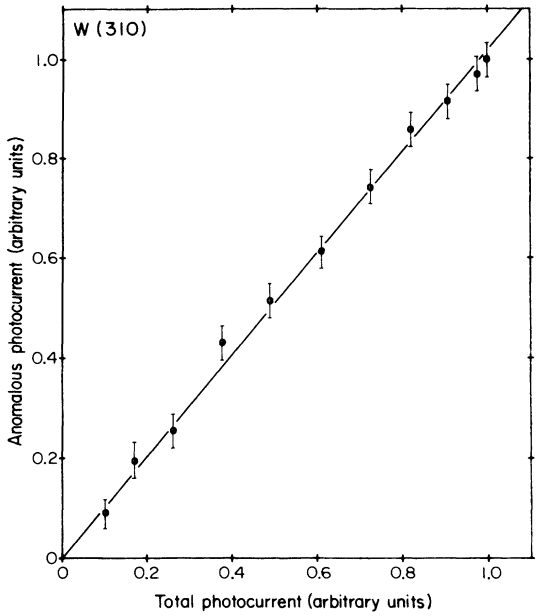


FIG. 5. The anomalous photofield-emission current plotted against total photocurrent density $J_p$ at a field of 0.34 V Å$^{-1}$, under conditions where $J_f \gg J_p$. The best-fit straight line passing through the origin is also shown.

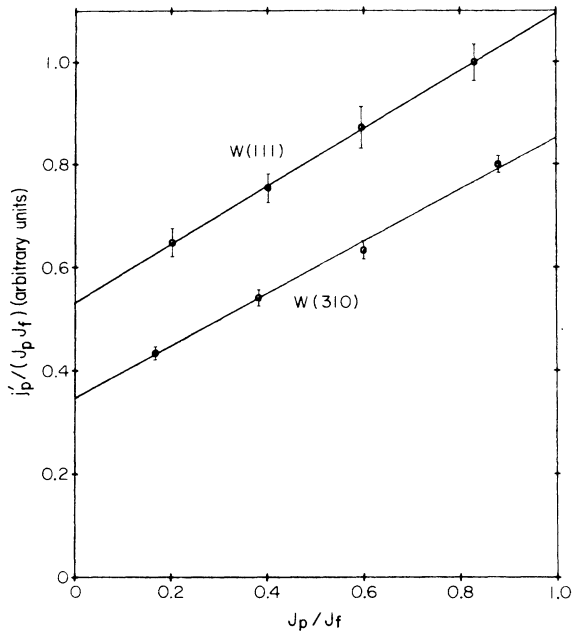


FIG. 6. The dependence on $J_p$ of the anomalous photocurrent under conditions where $J_p \sim J_f$. Equation (4) predicts that the data will fall on a straight line. From the plot the value of $\gamma_{pp}/\gamma$ may be determined. The upper curve is for the (111) region at 0.285 V Å$^{-1}$; the lower curve is for the (310) region at 0.27 V Å$^{-1}$.

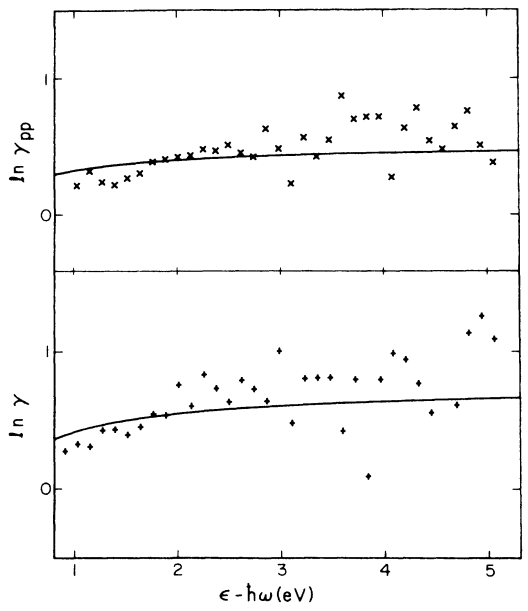


FIG. 7. Plot of the experimentally observed energy dependence of $\gamma$ at a field of 0.30 V Å$^{-1}$ and $\gamma_{pp}$ at a field of 0.23 V Å$^{-1}$. Data are of the emission from the (310) region with $p$-polarized illumination. The energy dependences calculated from Eq. (15) are shown as solid lines. The curves are shifted vertically by arbitrary amounts.

The energy dependence of $\gamma(\varepsilon)$ from the (310) region was measured at a fixed applied field. Combining Eq. (3) with Eq. (4), it follows that

$$\gamma(\varepsilon)=\frac{j'_p(\varepsilon)}{j'_f(\varepsilon-\hbar\omega;T_0)}\,\frac{J_f(T_0)^2}{J_p\{J_f(T_1)+[\gamma_{pp}(\varepsilon)/\gamma(\varepsilon)]J_p\}}\ , \quad (5)$$

where $T_0$ is the ambient temperature and $T_1$ is the tip temperature during illumination. Measurements were made to determine both $j'_f(\varepsilon)$ and $j'_p(\varepsilon)$. For the purpose of data analysis, it was assumed that $\gamma_{pp}/\gamma$ is independent of energy and equal to 1.5. Under the experimental conditions $J_f \simeq 50 J_p$, so that any errors introduced by this assumption are likely to be small. The results, plotted in Fig. 7, show that $\gamma$ depends only weakly upon energy.

Accurate determinations of $\gamma$(4.62 eV) were made for the (310) region using $p$-polarized illumination and for the (111) region in both $s$ and $p$ polarization. In all cases measurements were made of $j'_p$(4.62 eV) and $j'_f$(4.62 eV$-\hbar\omega;T_0$), and the TED's were measured in the vicinity of the peaks with and without laser illumination. During the course of each measurement, the drifts in $J_p$ and $J_f$ were less than 1.5%. The values of $\gamma$ obtained using Eq. (5) are reported in Table I. For the purpose of analysis, the measurements of $\gamma_{pp}$(4.62 eV)/$\gamma$(4.62 eV) reported above were used. For the measurement in $s$ polarization it was assumed that $\gamma_{pp}/\gamma = 1$. As in this measurement $J_f \simeq 250 J_p$, the error resulting from this assumption is likely to be small. $\gamma_{pp}$ may be found by combining the values of $\gamma$ with the measurements of $\gamma_{pp}/\gamma$. The results are also reported in Table I.

The energy dependence of $\gamma_{pp}$ was measured. It is shown above that $\gamma$ and $\gamma_{pp}$ are of the same order of magnitude, so if experiments are performed in conditions where $J_p \gg J_f$, it follows from Eq. (4) that $\gamma_{pp}(\varepsilon) \propto j_p(\varepsilon)/\kappa(\varepsilon-\hbar\omega)$. A measurement of $j_p(\varepsilon)$ was made at a field of 0.23 V Å$^{-1}$, and with $J_p \simeq 30 J_f$. As the

TABLE I. Comparison of the measured values of $\gamma$(4.62 eV) and $\gamma_{pp}$(4.62 eV) with the predictions of the Coulomb-interaction model. Data were taken at a field of $\sim$0.31 V Å$^{-1}$ and with a photon energy $\hbar\omega = 3.536$ eV.

| Region | Polarization | $\gamma$ (expt.) | $\gamma$ (theor.) | $\gamma_{pp}$ (expt.) | $\gamma_{pp}$ (theor.) |
|---|---|---|---|---|---|
| (310) | $p$ | 0.74(2) | 0.74 | 1.11(7) | 1.42 |
| (111) | $p$ | 0.65(2) | 0.67 | 0.60(8) | 1.28 |
| (111) | $s$ | 0.62(8) | 0.65 | | |

anomalous field-emission current at this field is very small, the energy dependence of $\kappa(\varepsilon-\hbar\omega)$ was deduced from the anomalous field emission at 0.30 V Å$^{-1}$. The results, plotted in Fig. 7, demonstrate that $\gamma_{pp}$ depends only weakly upon $\varepsilon$. This validates the assumption made above that $\gamma_{pp}/\gamma$ is almost independent of energy.

No attempt was made to detect a low-energy anomalous tail in PFE. If such a tail exists, and its strength is similar to that observed at high energy, then its detection would be masked by both the field-emission TED and by photofield-emitted electrons scattering off the analyzer walls.

## III. DISCUSSION

Anomalous tails have been observed in the TED's measured in both field and photofield emission. As the fraction of the current present in the tails depends only on the total current density, it seems likely that their origin lies outside of the field emitter. The possibility that the tails are a consequence of the instrumental response function is ruled out because it implies that the anomalous current in field emission would be proportional to $J_f$, whereas it is found experimentally that the anomalous current is proportional to $J_f^2$.

It was first observed by Boersh[20] that the energy distribution in an electron beam may reach a width of several electron volts even if thermal agitation at the source amounts to only a fraction of an electron volt. At the source, thermal agitation results in an isotropic velocity spread $\sim(k_BT/m)^{1/2}$. When the electrons are accelerated to a mean velocity **V**, the energy spread remains unaltered if collisions are neglected. This means that the axial velocity spread is reduced to $\sim[k_BT/(2mV)]$, while the transverse velocity spread remains constant. Hence the accelerated electron beam has an anisotropic distribution of velocity components. Collisions between the electrons will eventually mix the velocity-spread components and yield a velocity distribution that is isotropic in the moving frame. The resulting axial energy spread is $\sim(\frac{8}{3})^{1/2}(\frac{1}{2}k_BT\times\frac{1}{2}mV^2)^{1/2}$, which may be very much larger than the initial thermal energy spread $\sim k_BT$.

An additional source of energy broadening arises in the vicinity of beam crossovers (i.e., in regions where the beam is brought to a focus). In these regions, collisions can transfer transverse kinetic energy into axial kinetic energy. For essentially the same reasons as outlined above, this can lead to substantial energy broadening.[12,21]

Knauer[13] has argued that the steady Coulomb repulsion between electrons in the vicinity of the field emitter can also lead to substantial energy broadening. In what follows, this effect will be discussed on the basis of the geometry illustrated in Fig. 8. The total change in the kinetic energy of the *test* electron as a result of its Coulomb interaction with the *field* electron as it passes from the tip to the screen is given by

$$\Delta E = 1/(4\pi\varepsilon_0)\int_{z_0}^{z_s} e^2/b^2\cos\phi\, dz \ . \tag{6}$$

The spectrum of energy transfers will be calculated by assuming that the electrons are emitted uniformly in space and randomly in time from the surface of the hemispherical field emitter, and that the emission-current density is sufficiently low that, on the average, only one *field* electron plays a significant role. It will also be assumed that the electrostatic potential is radially symmetric, so that in the absence of interactions the trajectories are straight lines. Initially, it will be assumed that the emitted electrons are monoenergetic, and that the trajectories diverge so rapidly that the Coulomb interaction between electrons does not affect their trajectories.

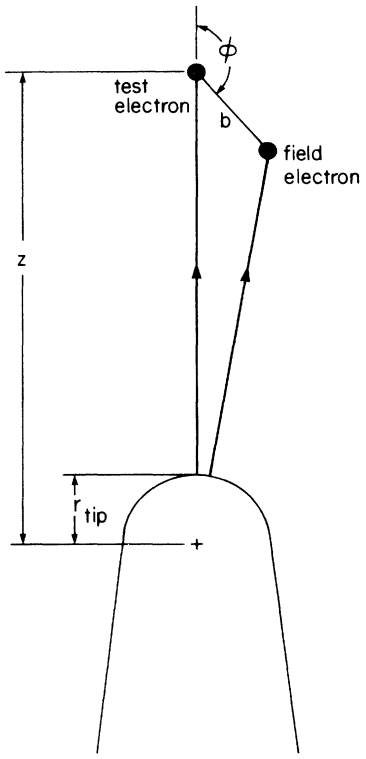


FIG. 8. Illustration of the geometry used to calculate the energy distribution resulting from the Coulomb interaction between electrons in the vacuum region close to the tip.

An analytic solution for the energy transfer is readily obtained[13] if it is further assumed that the external potential is constant, so that the electrons travel with a constant velocity $u$, and the time interval $\Delta t$ between the emission of the two electrons is sufficiently small that the approximation $\Delta t \ll r_{\rm tip}/u$ is valid. An integration over $\phi$ gives

$$\Delta E = \frac{1}{4\pi\varepsilon_0}\frac{e^2 r_{\rm tip}}{b_0^2}\frac{\sin\phi_0 - 1}{\cos\phi_0\sin\phi_0} \ . \tag{7}$$

For a pair of electrons with $b_0 = 100$ Å and $\phi_0 = 135°$, Eq. (7) gives $\Delta E = 1.68$ eV, a value that is typical of the energies associated with the anomalous emission tails. It should be noted that the transferred energy measured at the screen is very much larger than the potential energy of interaction between two electrons separated by 100 Å ($\sim$0.14 eV).

Consider field electrons having a given initial angle $\phi_0$ with respect to the test electron. It follows from Eq. (7) that, for such electrons,

$$\left[\frac{\partial b_0}{\partial \Delta E}\right]_{\phi_0} \propto (\Delta E)^{-3/2} . \tag{8}$$

The probability of a field electron being at an initial distance $b_0$ from the test electron is given by

$$dN = 2\pi n b_0^2 db_0 \sin\phi_0 d\phi_0 , \tag{9}$$

where $n$ is the particle density, and where it is assumed that $b_0 \ll r_{\text{tip}}$, so that the spatial variation of $n$ is unimportant. By combining Eqs. (8) and (9), it will be seen that

$$\left[\frac{\partial N}{\partial b_0}\right]_{\phi_0} \propto \Delta E^{-1} . \tag{10}$$

It follows that the emitted electrons will have an energy distribution of the form

$$j'(\Delta E;\phi_0) \propto \left[\frac{\partial N}{\partial \Delta E}\right]_{\phi_0} \propto \left[\frac{\partial N}{\partial b_0}\right]_{\phi_0}\left[\frac{\partial b_0}{\partial \Delta E}\right]_{\phi_0} \propto \Delta E^{-2.5} . \tag{11}$$

Thus the energy distribution follows a $\Delta E^{-5/2}$ law, irrespective of the angle $\phi_0$.

Numerical techniques were used to treat more realistically the effects of the Coulomb interaction. The potential was assumed to be that of an isolated sphere,

$$V(r) = V_s(1 - r_{\text{tip}}/r) , \tag{12}$$

where $V_s$ is the potential difference between the screen and the tip. The high-energy tail of the distribution resulting from a tip of radius 2000 Å with $V_s = 3000$ V was calculated, and was found to be

$$j'(\Delta E) = I(\Delta E) J_f^2 , \tag{13}$$

where

$$I(\Delta E) = (1.9\times 10^8)\Delta E^{-2.45}\ \text{A}^{-1}\,\text{Å}^2\,\text{eV}^{-1} , \tag{14}$$

and $\Delta E$ is in eV. In practice, the Coulomb repulsion between the electrons will perturb the electron trajectories, thereby reducing the transferred energy. A further calculation showed that, for $\Delta E \leq 4.0$ eV, Eq. (14) describes $I(\Delta E)$ for the resulting perturbed distribution to within 3%, that $I(8\text{ eV})$ was 70% of that given by Eq. (14) and that $I(12\text{ eV})$ was 18% of that given by Eq. (14). Additional calculations showed that increasing the energy of the test electron in the calculation by 3.5 eV resulted in changes in $I(\Delta E)$ of less than 0.5% for $0.2 < \Delta E < 7.0$ eV, demonstrating that the average energy transferred as a consequence of the Coulomb interaction does not depend significantly on the energy difference between the electrons involved.

On the basis of these considerations the measured TED is expected to be of the form

$$j(\varepsilon) = J_f \int_{-\infty}^{\infty} d\varepsilon'[\tilde{j}_f(\varepsilon') + \tilde{j}_p(\varepsilon')]I(\varepsilon - \varepsilon') + J_p \int_{-\infty}^{\infty} d\varepsilon'[\tilde{j}_f(\varepsilon') + \xi\tilde{j}_p(\varepsilon')]I(\varepsilon - \varepsilon') , \tag{15}$$

where $\tilde{j}(\epsilon)$ is the TED which would be measured in the absence of the Coulomb interaction, and $\xi$ is a numerical factor that allows for possible fluctuations of the photon flux in the laser beam. The dominant contribution to the integral in Eq. (15) comes from the energy range close to the peaks of the TED where the approximation $\tilde{j}(\epsilon) \simeq j(\epsilon)$ holds to high accuracy, so the application of Eq. (15) is straightforward. As $I(\Delta E)$ is much wider than the peaks in the TED predicted by the free electron theory, far from the peaks the Coulomb scattering tails may dominate the observed emission.

The probability of finding a pair of photons in the laser beam within a short time interval $\tau$, expressed relative to the square of the mean photon flux, is represented by the two-photon correlation function $\xi(\tau) \equiv \langle I(t)I(t+\tau)\rangle / \langle I(t)\rangle^2$, where $I$ is the beam intensity and $\langle\ \rangle$ denotes an average over time. The strength of the two-photoelectron tail, expressed relative to the square of the photoelectron current, will be proportional to $\xi(\tau)$. For significant Coulomb interaction to occur between a pair of photoelectrons, the two photons must be absorbed within a time interval of the order of $10^{-14}$ s. If it is assumed that the laser beam is a superposition of $N$ interfering longitudinal modes whose relative phases vary independently and randomly in time then the short time limit of $\xi$ is equal to $(2 - 1/N)$.[22] In the present experiments, the laser beam consists of approximately 30 longitudinal modes separated in frequency by $\sim 150$ MHz. Thus intensity fluctuations are expected to enhance the strength of the two-photoelectron tail, expressed relative to the square of the photoelectron current, by a factor $\xi \simeq 2$.

Energy transfer between electrons due to Coulomb interaction will be most significant in those regions where the electron density is high. Model calculations reveal that the electron density in the vicinity of the field emitter is a factor of $2\times 10^5$ times larger than it is at the first beam crossover in the electron-energy analyzer, and that in all other regions of the analyzer the electron density is negligibly small. As a result, the vast majority of the collisions which transfer significant energy between electrons will occur near the field emitter, and Eq. (15) should describe the net effect of Coulomb interactions.

The predictions of Eq. (15) can be compared with the experimental data. Since $\tilde{j}_f(\varepsilon)$ is proportional to $J_f$, it follows that in the absence of illumination $j_f'(\varepsilon)$ will be proportional to $J_f^2$, in agreement with experiment. Since $\tilde{j}_p(\varepsilon)$ is proportional to $J_p$, $j_p'(\varepsilon)$ will be proportional to $J_f J_p$ when $J_f \gg J_p$ and proportional to $J_p^2$ when $J_p \gg J_f$, also in agreement with experiment. Plotted in Fig. 3 are the results of evaluating Eq. (15) for two models of $I(\Delta E)$. The calculation which considers perturbations of the trajectories due to interaction describes with reasonable accuracy the energy dependences of the anomalous tails.

The Coulomb interaction model predicts both high- and low-energy tails in the TED's. A numerical integration of Eq. (15) gave $j_f'(-5.20\text{ eV})/j_f'(4.80\text{ eV}) = 0.84$, which is slightly smaller than the experimentally observed value of $0.98 \pm 0.05$. A numerical integration of Eq. (15) over the field-emission distribution measured at 0.32 V Å$^{-1}$ yielded $\kappa(1.08\text{ eV}) \simeq 1.6\times 10^8$ Å$^2$ A$^{-1}$ eV$^{-1}$. Bearing in mind the crudeness of the theoretical model and the large ex-

perimental uncertainty in estimating the absolute current density, this result is in reasonable agreement with the experimental value $\kappa \simeq 4\times 10^8$ Å$^2$ A$^{-1}$ eV$^{-1}$.

The Coulomb interaction model as expressed by Eq. (15) can be used to calculate the energy dependences of $\gamma$ and $\gamma_{pp}$. The comparison in Fig. 7 shows satisfactory agreement with experiment. In Table I the calculated values of $\gamma$ and $\gamma_{pp}$ for various conditions are compared with the experimental results. The calculation accurately predicts the strength of the one-photoelectron tail, but significantly overestimates the strength of the two-photoelectron tail.

The classical model for the Coulomb interaction between electrons just outside the emitting surface gives a generally satisfactory account of the experimental data. This conclusion is consistent with that of Bell and Swanson,[10] who demonstrated that gross departures from the predictions of the free-electron theory occur in field emission at current densities $\sim 10^3$ times greater than those used in the present work, and who suggested that these are caused by Coulomb interactions close to the tip. At the largest current densities used in the present work, the probability of a given electron being emitted sufficiently closely in time and space to another to yield an energy transfer in excess of 0.5 eV is $\sim 10^{-3}$. The corresponding probability of a given electron being emitted close to two other electrons is of order $(10^{-3})^2$, so that Coulomb scattering involving interactions between three or more electrons is relatively unimportant. By contrast, an analysis of the data of Bell and Swanson requires a consideration of these higher-order contributions.[13]

Gadzuk and Plummer[3] have suggested that the high-energy tails in field emission are caused by cascade processes initiated by the injection of "hot" holes (corresponding to the removal of electrons by field emission) into the metal. In this model a $J_f^2$ dependence occurs for $0<\varepsilon \ll \Phi$, where $\Phi$ is the work function, because the number of holes generated is proportional to $J_f$ and the probability of tunneling of the decay products is proportional to $J_f$. The cascade model predicts that the anomalous current at $\varepsilon \simeq \Phi$ will vary as $\sim J_f^{\eta}$, with $\eta = 2^{3/2} \simeq 2.8$, in contrast to the $J_f^2$ dependence observed experimentally. The cascade model also predicts that the anomalous tail in the TED will vary as $\varepsilon^{-3}$, which is significantly different from the $\sim \varepsilon^{-2.6}$ dependence observed experimentally. Further, the cascade model offers no explanation for the success of Eq. (15) in describing the relative strengths of the anomalous field- and photofield-emission tails. It is concluded that hole-cascade processes are not responsible for the anomalous tails.

Several authors have discussed the role of the uncertainty principle in field emission, and have considered in some detail the tunneling lifetime of field-emitted electrons.[8,9] According to the ideas outlined in Ref. 8, the energies of the electron states from which field emission is observed are broadened by an amount $\Delta \simeq \hbar/\tau$, where $\tau$ is a tunneling lifetime. This leads to a measured TED of the form

$$j(\varepsilon) = (1/\pi) \int_{-\infty}^{\infty} d\varepsilon' \tilde{j}(\varepsilon') \Delta(\varepsilon') / [(\varepsilon - \varepsilon')^2 + \Delta(\varepsilon')^2] , \tag{16}$$

where $\tilde{j}(\varepsilon)$ is the TED calculated without taking into account the tunneling lifetime. It was suggested that $\Delta(\varepsilon) = \Delta_0 e^{(-c+\varepsilon/d)}$, where $c$ and $d$ are defined as in Eq. (2), and where $\Delta_0$ is a weak function of energy. The dominant contribution to the integral in Eq. (16) comes from the energy range close to the peaks of the TED where the approximation $\tilde{j}(\varepsilon) \simeq j(\varepsilon)$ is accurate. The energy dependence of the field-emission tail at 0.36 V Å$^{-1}$, calculated from Eq. (16), is included in Fig. 3. For the field-emission experiments performed at a field of 0.32 V Å$^{-1}$, one obtains, from Eq. (10) of Ref. 8, $\tau(\varepsilon'=0) \simeq 2\times 10^{-10}$ s, from which it follows that $\Delta_0 e^{-c} \simeq 3\times 10^{-6}$. A numerical integration of Eq. (16) over the corresponding field-emission TED gives an estimate of $j(\varepsilon = 1.08$ eV$)/J_f = 1.1\times 10^{-6}$ eV$^{-1}$, which is approximately 2% of the value observed experimentally. In contrast, at $\varepsilon \simeq 17$ eV the anomalous current predicted by the tunneling-lifetime model is approximately 50 times larger than the measured current.

The Coulomb-interaction model is superior to the tunneling-lifetime model in its predictions of the magnitude and the energy dependence of the anomalous current in field emission. The Coulomb-interaction model also accounts quantitatively for the observations in photofield emission. It is not yet known whether the photofield-emission data can be understood in terms of the tunneling-lifetime model. In the range $\varepsilon \simeq 17$ eV the Coulomb-interaction model predicts the anomalous current to within a factor of 4, while the tunneling-lifetime model predicts an anomalous current that is too large by a factor of 50. This implies that the value of the tunneling lifetime to be used in applying Eq. (16) must be at least 50 times longer than that suggested in Ref. 8.

There are two significant discrepancies between the predictions of the Coulomb interaction model and the experimental data. The discrepancies between the calculated energy dependence and the experimental data (Fig. 3) could be a consequence of the simplified geometry assumed in the model calculation. However, this explanation cannot account for the discrepancies in the values of $\gamma_{pp}$. The discrepancies in $\gamma_{pp}$ could be caused by correlations in the phases of the longitudinal modes in the laser, which would invalidate the assumption $\xi = 2$. Measurements using a single-mode laser should be carried out to eliminate this source of uncertainty in the interpretation of the data.

Other possible sources of discrepancy are errors in the assumption that the emission of electrons is uniform in space and random in time. Consider the assumption that the emission is uniform in space. The model calculation shows that if more than 1.1 eV of energy is transferred between electrons as a result of the Coulomb interaction, then at the tip the distance between the electron trajectories must be less than 85 Å. Hence only electrons emitted within approximately 85 Å of the region of observation contribute significantly to the observed scattering. Visual observations indicate that in both field and photofield emission the current density is uniform to better than 10% within 120 Å of the (111) and (310) regions. Since the diameter of the region of the tip which is projected onto the probe hole is $\sim 80$ Å, these results sug-

gest that the probe hole current is a reasonable measure of the current density that is responsible for the Coulomb scattering in both field and photofield emission. Thus if nonuniform emission is responsible for the discrepancy between the observed and calculated values of $\gamma_{pp}$, it can only be due to nonuniformities on a length scale smaller than the $\sim$30-Å resolution[19] of the field-emission microscope.

The form of the Coulomb-scattering tail in the field-emission TED's provides information about the electron-emission process on a timescale of $10^{-15}$ s. When the emission-current density is $1.5\times10^{-13}$ A Å$^{-2}$, the average time interval between the emission of two successive electrons from a region of radius 100 Å on the tip is $3\times10^{-11}$ s. Consider the possibility that 1 part in $10^4$ of the emission current is due the emission of correlated pairs of electrons, such that the initial distance between the electrons is random but less than 100 Å, and that the time interval between the emission of the two electrons is random but less than $\Delta t = 5\times10^{-16}$ s. Numerical calculations show that strength of the anomalous tail would be enhanced relative to that predicted by the random-emission model by a factor of 3 at $\varepsilon=1$ eV and by a factor of 12 at $\varepsilon=8$ eV. The corresponding enhancements for $\Delta t = 4\times10^{-15}$ s would be by factors of 2.5 and 3, respectively. Clearly, both the shape and strength of the anomalous tail are very sensitive to departures from spatial and temporal randomness in electron emission. Nevertheless, the reasonable agreement between experiment and the predictions of the random-emission model suggests that, in tungsten, departures from random emission are small.

Various effects may lead to a correlation in the time between the emission of electrons on very short timescales. One possibility is the occurrence of multiple-electron tunneling.[2,23,24] Another possibility is suggested by the following semiclassical argument. Immediately after an electron escapes into the vacuum, the effective height of the surface-potential barrier for the electrons remaining inside the metal increases momentarily because of the potential of the escaping electron. The momentary fractional reduction in the electron-emission probability will be larger in field emission than in photofield emission, because field emission occurs via tunneling while photofield emission occurs primarily via emission at energies close to the peak of the surface potential barrier. As a result the interaction between photofield-emitted electrons will be greater on average than that between field-emitted electrons. This suggests that the experimental value of $\gamma_{pp}/\gamma$ will be larger than that predicted on the basis of random emission. By contrast, the measurements give values of $\gamma_{pp}/\gamma$ smaller than that predicted on the basis of random emission. It is not yet clear whether this semiclassical idea will be supported by a fully quantum mechanical treatment.

The existence of Coulomb-scattering tails has important practical implications. Below a certain energy level (2 eV or so below $E_f$) the field-emission current will be masked by the low-energy Coulomb-scattering tail. Moreover, the PFE current will be masked by the high-energy tail, particularly at relatively large applied electric fields. In these cases, the photofield-emission TED is, to a good approximation, equal to the difference between a distribution measured with the tip illuminated and a distribution measured in the absence of illumination. Finally, in the conditions of the present experiments a significant current of photoelectrons is observed at energies greater than $1.5\hbar\omega$ above the Fermi level, the emission current being proportional to $J_p^2$. In this regime, photofield emission followed by Coulomb scattering in the vacuum is the dominant two-photon process.

## IV. CONCLUSIONS

An anomalous high-energy tail has been observed in the measured total-energy distribution (TED) in photofield emission from tungsten. The current in this tail is very nearly proportional to the product of the photofield-emission-current density and the total-emission-current density. Similar high- and low-energy tails in the TED's in field emission, which have previously been reported by several groups, are also observed. The absolute strength of the anomalous field-emission tail was measured, as were the energy dependences of the high-energy anomalous tails in both field and photofield emission. The strength of the high-energy field-emission tail was compared both to the low-energy field-emission tail and to the photofield-emission tail.

The experimental observations are generally consistent with the predictions of a classical calculation which considers the energy transfer that results from Coulomb scattering of electrons in the vacuum near the field emitter. It is pointed out that the Coulomb interaction acts as a probe of the correlated emission of electrons on the time scale of $10^{-15}$ s. Over the range of emission current densities studied in the present work ($10^5$–$10^8$ A m$^{-2}$), no significant role is played by the various internal mechanisms that have previously been proposed to account for the anomalous field emission tails.

## ACKNOWLEDGMENTS

This research was supported in part by grants from the National Sciences and Engineering Research Council of Canada.

[1]R. D. Young, Phys. Rev. **113**, 110 (1959).
[2]C. Lea and R. Gomer, Phys. Rev. Lett. **25**, 804 (1970).
[3]J. W. Gadzuk and E. W. Plummer, Phys. Rev. Lett. **26**, 92 (1971).
[4]M. Isaacson and R. Gomer, Appl. Phys. **15**, 253 (1978).
[5]H. F. Kempin, K. Klapper, and G. Ertl, Rev. Sci. Instrum. **49**, 1285 (1978).
[6]C. J. Workowski, J. Phys. E **13**, 67 (1980).
[7]P. E. Batson, Ultramicrosc. **18**, 125 (1985).
[8]J. W. Gadzuk and A. A. Lucas, Phys. Rev. B **7**, 4770 (1973).
[9]X. Aymerich-Humet and F. Serra-Mestres, Phys. Lett. **78A**, 312 (1980).

[10]A. E. Bell and A. W. Swanson, Phys. Rev. B **19**, 3353 (1979).
[11]M. Essig and J. Geiger, Appl. Phys. **25**, 115 (1981).
[12]W. Knauer, J. Vac. Sci. Technol. **16**, 1676 (1979).
[13]W. Knauer, Opt. (Stuttgart) **54**, 335 (1981).
[14]D. Venus and M. J. G. Lee, Rev. Sci. Instrum. **56**, 1206 (1985).
[15]R. H. Good and E. W. Müller, in *Handbuch der Physik,* edited by S. Flügge (Springer-Verlag, Berlin, 1956), Vol. 27, p. 176.
[16]D. Venus and M. J. G. Lee, Surf. Sci. **125**, 452 (1982).
[17]A. Bagchi, Phys. Rev. B **10**, 542 (1974).
[18]C. Schwartz and M. W. Cole, Surf. Sci. **115**, 290 (1980).
[19]R. Gomer, *Field Emission and Field Ionization* (Harvard University Press, Cambridge, Mass., 1961).
[20]H. Boersch, Z. Phys. **139**, 115 (1954).
[21]B. Zimmerman, Adv. Electron Phys. **29**, 257 (1970).
[22]F. Sanchez, Nuovo Cimento B **27**, 305 (1975).
[23]J. W. Gadzuk and E. W. Plummer, Rev. Mod. Phys. **45**, 487 (1973).
[24]K. L. Ngai, Phys. Status Solidi B **53**, 309 (1972).